Rheol Acta (2012) 51:497–510
DOI 10.1007/s00397-012-0618-x

ORIGINAL CONTRIBUTION

Perturbation solutions of weakly compressible Newtonian Poiseuille flows with Navier slip at the wall

Stella Poyiadji · Georgios C. Georgiou · Katerina Kaouri · Kostas D. Housiadas

Received: 7 October 2011 / Revised: 13 January 2012 / Accepted: 17 January 2012 / Published online: 8 February 2012

Abstract We consider both the planar and axisymmetric steady, laminar Poiseuille flows of a weakly compressible Newtonian fluid assuming that slip occurs along the wall following Navier's slip equation and that the density obeys a linear equation of state. A perturbation analysis is performed in terms of the primary flow variables using the dimensionless isothermal compressibility as the perturbation parameter. Solutions up to the second order are derived and compared with available analytical results. The combined effects of slip, compressibility, and inertia are discussed with emphasis on the required pressure drop and the average Darcy friction factor.

Keywords Newtonian flow · Poiseuille flow · Compressibility · Slip · Perturbation solution · Darcy friction factor

S. Poyiadji · G. C. Georgiou (✉)
Department of Mathematics and Statistics,
University of Cyprus, P.O. Box 20537,
1678 Nicosia, Cyprus
e-mail: georgios@ucy.ac.cy

S. Poyiadji
e-mail: map4sp1@ucy.ac.cy

K. Kaouri
Department of Computer Science,
Intercollege Limassol, Ag. Fylaxeos 92,
3507 Limassol, Cyprus
e-mail: katerina.kaouri@gmail.com

K. D. Housiadas
Department of Mathematics,
University of the Aegean, Karlovassi, Samos 83200, Greece
e-mail: housiada@aegean.gr

Introduction

In a recent paper (Taliadorou et al. 2009), we derived second-order perturbation solutions of both the planar and axisymmetric Poiseuille flows of weakly compressible Newtonian fluids using a methodology in which the primary flow variables, i.e., the velocity components and pressure, are perturbed, a linear equation of state is employed, and compressibility serves as the perturbation parameter. The same solutions were derived by Venerus (2006) and Venerus and Bugajsky (2010) respectively for the axisymmetric and planar flow problems using a streamfunction/vorticity formulation. We have recently extended the primary-variable methodology to derive perturbation solutions of the planar and axisymmetric Poiseuille flows of a weakly compressible Oldroyd-B fluid (Housiadas and Georgiou 2011; Housiadas et al. 2012). The aforementioned references provide useful reviews of previous perturbation and other approximate solutions of the flow problems under consideration.

The objective of the present paper is to extend our previous work for a Newtonian liquid allowing linear slip at the wall in order to study the combined effects of weak compressibility, slip and inertia. The importance of slip in a variety of macroscopic flows and processes has been emphasized in numerous studies in the past few decades (Denn 2001; Hatzikiriakos and Migler 2005, and references therein). Strong interest has also been recently generated due to the effects of slip in microfluidic applications (Stone et al. 2004). Slip of molten polymers has been recently reviewed by Hatzikiriakos (2012).

In flows of liquids, such as polymer melts and waxy crude oils, compressibility may become important

when the liquids are processed at high pressures, which is the case with polymer extrusion (Hatzikiriakos and Dealy 1992; Piau and El 1994) or with flow through long tubes (Vinay et al. 2006; Wachs et al. 2009). The stick-slip polymer extrusion instability, referring to the sustained pressure and flow rate oscillations observed under constant throughput, is attributed to the combination of compressibility with nonmonotonic slip laws relating the wall shear stress to the slip velocity (Hatzikiriakos and Dealy 1992; Georgiou 2005) as confirmed by one-dimensional phenomenological models (Dubbeldam and Molenaar 2003) as well numerical simulations (Taliadorou et al. 2007). Tang and Kalyon (2008a, b) also developed a mathematical model describing the time-dependent pressure-driven flow of compressible polymeric liquids subject to pressure-dependent slip and reported that undamped periodic pressure oscillations in pressure and mean velocity are observed when the boundary condition changes from weak to strong slip. Taliadorou et al. (2008) reported extrusion simulations showing that severe compressibility combined with inertia may lead to stable steady-state free surface oscillations, similar to those observed experimentally with liquid foams. Mitsoulis and Hatzikiriakos (2009) carried out steady flow simulations of polytetrafluoroethylene (PTFE) paste extrusion under severe slip taking into account the significant compressibility of these pastes.

The above material flows are weakly compressible, which means that the Mach number, *Ma*, is low, i.e. $Ma << 1$. The latter number is defined as the ratio of the characteristic speed of the flow to the speed of sound in the fluid. Georgiou and Crochet (1994) pointed out that taking into account the weak compressibility of the fluid may not have an effect on the steady flow solution but changes dramatically the flow dynamics. Similarly, Felderhof and Ooms (2011) studied the flow of a viscous compressible fluid in a circular tube generated by an impulsive point source and reported that compressibility has a significant effect on the flow dynamics in confined geometries.

The combination of slip with compressibility is also very important in rarefied gas flows through microchannels and need to be taken into account in the micro-electro-mechanical systems technology (Beskok and Karniadakis 1999; Zhang et al. 2009). There are of course some important differences from the liquid flow problem under consideration: (a) the continuum assumption may not be valid and slip velocity is expressed in terms of the Knudsen number *Kn* (the ratio of the mean free path of the gas to the characteristic dimension of the tube); (b) the ideal gas law is used instead of the linear equation of state; and (c) the flow is non-isothermal. Arkilic and Schmidt (1997) and, more recently, Qin et al. (2007) derived perturbation approximations for compressible gas flow in microchannels with slip at the wall using the aspect ratio as the perturbation parameter. According to conventional theory, continuum-based models for channels apply as long as the Knudsen number is lower than 0.01 (Kohl et al. 2005). On the other hand, according to Venerus and Bugajsky (2010), effects of slip in microchannels can be neglected for Knudsen numbers less than 0.001. Therefore, the present analysis concerns not only flows of compressible liquids with slip at the wall but also gas flows for $0.001 < Kn < 0.01$.

The paper is organized as follows: first, the governing equations and boundary conditions for the steady, compressible plane Poiseuille flow with slip at the wall are presented; the results for the axisymmetric flow are provided in the Appendix. Both the state and slip equations are assumed to be linear. Then, the perturbation method in terms of the primary variables with the isothermal compressibility as the perturbation parameter is outlined and a solution is derived up to the second order. Explicit analytical solutions for the two non-zero velocity components, the pressure, and the density are obtained. Finally, the results are analyzed and discussed with the emphasis given on the combined effects of slip and compressibility on the pressure drop and the Darcy friction factor.

Governing equations

We consider the steady, laminar plane Poiseuille flow of a Newtonian fluid in a slit of length L^* and width $2H^*$ in Cartesian coordinates (x^*, y^*), as shown in Fig. 1. Note that throughout the text, dimensional quantities are denoted by a star; symbols without a star denote dimensionless variables and numbers. It is

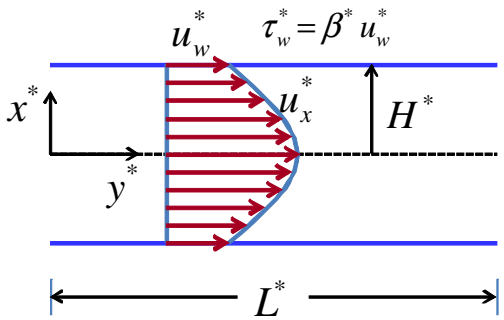

Fig. 1 Geometry and symbols for plane Poiseuille flow with slip along the wall

assumed that slip occurs along the wall according to a linear slip equation,

$$\tau_w^* = \beta^* u_w^*, \tag{1}$$

where τ_w^* is the wall shear stress, β^* is the constant slip coefficient, and u_w^* is the slip velocity. The limiting case $\beta^* \to \infty$ corresponds to the no-slip boundary condition ($u_w^* \to 0$), whereas $\beta^* = 0$ corresponds to the theoretical case of full slip in which the velocity profile is plug.

Let us consider first the incompressible, one-dimensional flow under constant pressure gradient, $(-\partial p^*/\partial x^*)$. The velocity $u_x^*(y^*)$ is given by

$$u_x^*(y^*) = \frac{H^*}{\beta^*}\left(-\frac{\partial p^*}{\partial x^*}\right) + \frac{1}{2\eta^*}\left(-\frac{\partial p^*}{\partial x^*}\right)\left(H^{*2} - y^{*2}\right) \tag{2}$$

where η^* is the constant viscosity. Obviously, the slip velocity is given by

$$u_w^* = u_x^*(H^*) = \frac{H^*}{\beta^*}\left(-\frac{\partial p^*}{\partial x^*}\right) \tag{3}$$

If the fluid is compressible, the flow becomes bidirectional and the two velocity components, u_x^* and u_y^*, are in general functions of both x^* and y^*. The isothermal compressibility is a measure of the ability of the material to change its volume under applied pressure at constant temperature. This is defined by

$$\kappa^* \equiv -\frac{1}{V_0^*}\left(\frac{\partial V^*}{\partial p^*}\right)_{p_0^*, T_0^*} \tag{4}$$

where V^* is the specific volume and V_0^* is the specific volume at the reference pressure, p_0^*, and temperature, T_0^*. Assuming that κ^* is constant, the above equation can be integrated yielding an exponential equation of state. In the present work, however, we employ a linear equation of state,

$$\rho^* = \rho_0^*\left[1 + \kappa^*\left(p^* - p_0^*\right)\right], \tag{5}$$

where ρ^* is the density and ρ_0^* is the density at the reference pressure and temperature. Equation 5 approximates well the exponential equation of state for small values of κ^* and for small pressures. The value of κ^* is of the order of 0.001 MPa^{-1} for molten polymers (Hatzikiriakos and Dealy 1994) and increases by an order of magnitude (0.0178–0.0247 MPa^{-1}) in the case of PTFE pastes (Mitsoulis and Hatzikiriakos 2009). Mitsoulis and Hatzikiriakos (2009) suggest that for weakly compressible flows, the values of κ^* range between 0 (incompressible fluids) and 0.02 MPa^{-1} (slightly to moderately compressible materials). The linear equation of state can also be viewed as a special case of the well-established Tait equation and its variants for liquids and polymer melts (Guaily et al. 2011).

In order to dedimensionalize the governing equations and the boundary conditions of the flow, we scale x^* by the length of the channel L^*, y^* by the channel half-width H^*, the density ρ^* by the reference density ρ_0^*, the horizontal velocity, u_x^*, by the mean velocity at the channel exit U^*,

$$U^* \equiv \frac{\dot{M}^*}{\rho_0^* H^* W^*}$$

where $\dot{M}^*$ is the mass flow rate and W^* is the unit length in the z^*-direction, and the transversal velocity, u_y^*, by $U^* H^*/L^*$. The Mach number is defined by

$$Ma \equiv \frac{U^*}{\sigma^*} \tag{6}$$

where

$$\sigma^* \equiv \left[\gamma\left(\frac{\partial p^*}{\partial \rho^*}\right)_{T^*}\right]^{1/2} = \left(\frac{\gamma}{\kappa^* \rho_0^*}\right)^{1/2} \tag{7}$$

is the speed of sound in the fluid, γ being the heat capacity ratio or adiabatic index ($\gamma \equiv c_p^*/c_v^*$).

With the above scalings, the dimensionless slip equation becomes

$$\tau_w = B\, u_w \tag{8}$$

where all variables are now dimensionless and B is the slip number defined by

$$B \equiv \frac{\beta^* H^*}{\eta^*} \tag{9}$$

The dimensionless velocity profile in the case of incompressible flow becomes

$$u_x(y) = \frac{3}{B+3} + \frac{3B}{2(B+3)}\left(1 - y^2\right) \tag{10}$$

or

$$u_x(y) = \frac{\bar{B}}{B} + \frac{\bar{B}}{2}\left(1 - y^2\right) \tag{11}$$

where

$$\bar{B} \equiv \frac{3B}{B+3} \tag{12}$$

is an auxiliary slip number. In the no-slip limit, $B \to \infty$ and $\bar{B} \to 3$. Therefore,

$$u_x^{(0)}(y) = \frac{3}{2}\left(1 - y^2\right) \tag{13}$$

which is the standard velocity profile for incompressible flow with no slip at the wall.

By demanding that the dimensionless pressure drop in the case of incompressible flow with no slip at the wall be equal to 1, the pressure scale should be $3\eta^* L^* U^*/H^{*2}$. The dimensionless form of the equation of state (Eq. 5) is then

$$\rho = 1 + \varepsilon p \tag{14}$$

where

$$\varepsilon \equiv \frac{3\kappa^*\eta^* L^* U^*}{H^{*2}} \tag{15}$$

is the compressibility number. The Mach number takes the form

$$Ma = \sqrt{\frac{\varepsilon\alpha\, Re}{3\gamma}} \Leftrightarrow \varepsilon = \left(\frac{3\gamma}{\alpha Re}\right) Ma^2 \tag{16}$$

The present work deals with weakly compressible flows, e.g. $Ma < 0.3$. Assuming that γ is of the order of unity, there must be $\varepsilon\alpha Re < 0.27$.

The dimensionless forms of the continuity and the x-and y-momentum equations in the case of compressible Poiseuille flow under the assumptions of zero bulk velocity and zero gravity (Taliadorou et al. 2009) are

$$\frac{\partial(\rho u_x)}{\partial x} + \frac{\partial(\rho u_y)}{\partial y} = 0 \tag{17}$$

$$\alpha Re\,\rho\left(u_x\frac{\partial u_x}{\partial x} + u_y\frac{\partial u_x}{\partial y}\right) = -3\frac{\partial p}{\partial x} + \alpha^2\frac{\partial^2 u_x}{\partial x^2} + \frac{\partial^2 u_x}{\partial y^2} + \frac{\alpha^2}{3}\left(\frac{\partial^2 u_y}{\partial x\partial y} + \frac{\partial^2 u_x}{\partial x^2}\right) \tag{18}$$

$$\alpha^3 Re\rho\left(u_x\frac{\partial u_y}{\partial x} + u_y\frac{\partial u_y}{\partial y}\right) = -3\frac{\partial p}{\partial y} + \alpha^4\frac{\partial^2 u_y}{\partial x^2} + \alpha^2\frac{\partial^2 u_y}{\partial y^2} + \frac{\alpha^2}{3}\left(\frac{\partial^2 u_x}{\partial x\partial y} + \frac{\partial^2 u_y}{\partial y^2}\right) \tag{19}$$

where

$$Re \equiv \frac{\rho_0^* H^* U^*}{\eta^*} \tag{20}$$

is the Reynolds number, and

$$\alpha \equiv \frac{H^*}{L^*} \tag{21}$$

is the aspect ratio of the channel.

As for the boundary conditions, the usual symmetry conditions are applied along the symmetry plane; along the wall u_x obeys the slip equation (Eq. 8) while u_y vanishes. Moreover, the pressure at the upper right corner of the flow domain is set to zero and the mass flow rate at the exit plane should be equal to 1. Therefore, the conditions that close the system of the governing equations are the following:

$$\frac{\partial u_x}{\partial y}(x, 0) = u_y(x, 0) = 0 \tag{22}$$

$$-\frac{\partial u_x}{\partial y}(x, 1) = B\,u_x(x, 1) \quad \text{and} \quad u_y(x, 1) = 0 \tag{23}$$

$$p(1, 1) = 0 \tag{24}$$

$$\int_0^1 \rho u_x dy\Big|_{x=1} = 1 \tag{25}$$

As in Venerus (2006) and Taliadorou et al. (2009), no boundary conditions for the velocity are imposed at the entrance and exit planes ($x = 0$ and 1). The flow problem defined by Eqs. 14, 17–19 and 22–25 involves four dependent variables, u_x, u_y, p, and ρ, and four dimensionless numbers: ε, B, Re and α. Even though the density ρ can be eliminated by means of Eq. 14, it is kept in order to facilitate the derivation of the perturbation solution.

Perturbation solution

The present work deals with weakly compressible flows, that is the Mach number is small, typically $Ma < 0.3$. From Eq. 16, it is deduced that as long as Ma is small and $\gamma/(\alpha Re)$ is of the order of unity or smaller, the compressibility number ε is also a small number that can be used as the perturbation parameter. We thus perturb all primary variables, u_x, u_y, p, and ρ, as follows:

$$\begin{aligned} u_x &= u_x^{(0)} + \varepsilon u_x^{(1)} + \varepsilon^2 u_x^{(2)} + O\left(\varepsilon^3\right) \\ u_y &= u_y^{(0)} + \varepsilon u_y^{(1)} + \varepsilon^2 u_y^{(2)} + O\left(\varepsilon^3\right) \\ p &= p^{(0)} + \varepsilon p^{(1)} + \varepsilon^2 p^{(2)} + O\left(\varepsilon^3\right) \\ \rho &= \rho^{(0)} + \varepsilon\rho^{(1)} + \varepsilon^2\rho^{(2)} + O\left(\varepsilon^3\right) \end{aligned} \tag{26}$$

By substituting expansions (Eq. 26) into the governing Eqs. 14, 17–19 and also in the boundary conditions 22–25 and by collecting the terms of a given order in ε the corresponding perturbation equations and the

boundary conditions are obtained. These can be found in Taliadorou et al. (2009) who present the more general case with non-zero bulk viscosity. As for the slip equation, it can easily be shown that

$$-\frac{\partial u_x^{(k)}}{\partial y}(x,1) = B\,u_x^{(k)}(x,1), \quad k = 0,1,2,\ldots \tag{27}$$

where k is the order of the perturbation. The derivation of the leading-order solutions, which is based on the assumption that the transverse velocity u_y is zero, is straightforward and the methodology is described in detail by Poyiadji (2012). The perturbation solution of the flow problem up to second order is:

$$\begin{aligned}
u_x = {} & \frac{\overline{B}}{2B}\left(B+2-By^2\right) \\
& + \varepsilon\left[-\frac{\overline{B}^2}{6B}\left(B+2-By^2\right)(1-x) - \frac{\alpha Re\overline{B}^4}{7560B^2}\left[5B^2+45B+98-3\left(11B^2+77B+140\right)y^2+35\left(B^2+5B+6\right)y^4-7\left(B^2+3B\right)y^6\right]\right] \\
& + \varepsilon^2\left[\frac{\overline{B}^3}{12B}\left(B+2-By^2\right)(1-x)^2 - \frac{\alpha Re\overline{B}^5}{7560B^4}\right. \\
& \quad \times\left[19B^4+171B^3+658B^2+1260B+840+3\left(3B^4+21B^3-140B\right)y^2-35\left(B^4+5B^3+6B^2\right)y^4+7\left(B^4+3B^3\right)y^6\right] \\
& \quad \times(1-x) - \frac{\alpha^2\overline{B}^4}{648B^2}\left[B^2+3B+8+2\left(B^2+7B\right)y^2-3\left(B^2+3B\right)y^4\right] - \frac{\alpha^2Re^2\overline{B}^7}{314344800B^5} \\
& \quad \times\left[2193B^5+35088B^4+221641B^3+731346B^2+1409100B+1358280\right. \\
& \qquad -4\left(2839B^5+39746B^4+239316B^3+803880B^2+1576575B+1455300\right)y^2 \\
& \qquad +2310\left(B^5+12B^4+111B^3+602B^2+1470B+1260\right)y^4+924\left(13B^5+130B^4+448B^3+560B^2+105B\right)y^6 \\
& \qquad \left.\left.-5775\left(B^5+8B^4+21B^3+18B^2\right)y^8+616\left(B^5+6B^4+9B^3\right)y^{10}\right]\right] + O\left(\varepsilon^3\right)
\end{aligned} \tag{28}$$

$$u_y = \varepsilon^2\frac{\alpha Re\overline{B}^5}{11340B^2}y\left(1-y^2\right)\left[5B^2+45B+98-2\left(3B^2+16B+21\right)y^2+\left(B^2+3B\right)y^4\right] + O\left(\varepsilon^3\right) \tag{29}$$

$$\begin{aligned}
p = {} & \frac{\overline{B}}{3}(1-x) + \varepsilon\left[-\frac{\overline{B}^2}{18}(1-x)^2 + \frac{\alpha Re\overline{B}^4}{315B^3}\left(2B^3+14B^2+35B+35\right)(1-x) + \frac{\alpha^2\overline{B}^2}{54}\left(1-y^2\right)\right] \\
& + \varepsilon^2\left[\frac{\overline{B}^3}{54}(1-x)^3 - \frac{\alpha Re\overline{B}^5}{945B^3}\left(4B^3+28B^2+70B+70\right)(1-x)^2 - \frac{\alpha^2\overline{B}^4}{486B^2}\left[11B^2+53B+72-3\left(B^2+3B\right)y^2\right](1-x)\right. \\
& \quad + \frac{\alpha^2Re^2\overline{B}^7}{29469825B^6}\left(3044B^6+42616B^5+267036B^4+951720B^3+1964655B^2+2182950B+1091475\right)(1-x) \\
& \quad + \frac{\alpha^3Re\overline{B}^5}{204120B^3}\left[97B^3+889B^2+2310B+1260-3\left(79B^3+553B^2+1120B+420\right)y^2\right. \\
& \qquad \left.\left.+175\left(B^3+5B^2+6B\right)y^4-35\left(B^3+3B^2\right)y^6\right]\right] + O\left(\varepsilon^3\right)
\end{aligned} \tag{30}$$

$$\rho = 1+\varepsilon\frac{\overline{B}}{3}(1-x) + \varepsilon^2\left[-\frac{\overline{B}^2}{18}(1-x)^2+\frac{\alpha Re\overline{B}^4}{315B^3}(2B^3+14B^2 +35B+35)(1-x)+\frac{\alpha^2\overline{B}^2}{54}\left(1-y^2\right)\right]+O\left(\varepsilon^3\right) \quad (31)$$

Letting $B \to \infty$ we get the solution obtained by Taliadorou et al. (2009) and Venerus and Bugajsky (2010) for flow with no-slip at the wall. The perturbation solution of the axisymmetric flow is given in the Appendix.

The volumetric flow rate,

$$Q(x) \equiv \int_0^1 u_x(x,y)\,dy \quad (32)$$

is given by

$$Q(x) = 1-\varepsilon\frac{\overline{B}}{3}(1-x) + \varepsilon^2\left[\frac{\overline{B}^2}{6}(1-x)^2-\frac{\alpha Re\overline{B}^4}{315B^3}\left(2B^3+14B^2+35B+35\right)\times(1-x)-\frac{\alpha^2\overline{B}^3}{405B}(2B+5)\right]+O\left(\varepsilon^3\right) \quad (33)$$

Discussion

Let us first discuss the effect of the slip number on the two velocity components. In creeping flow ($Re = 0$), the transverse velocity component, u_y, is zero at second order. The effect of the slip number B on the transverse velocity is shown in Fig. 2. The transverse velocity is reduced as the slip number is reduced from infinity (no slip) to zero (full-slip). As slip becomes stronger the velocity in the flow direction tends to become more uniform and thus the flow tends to become one-dimensional. Given that the transverse velocity component is always positive (Eq. 29), the streamlines of the flow under study are either horizontal or have a slight positive slope which reaches its maximum value roughly in the middle of the y-interval [0,1]. The effect of slip on the transverse velocity component is more clearly illustrated in Fig. 3 where the reduced mean value,

$$\frac{\overline{u}_y}{\alpha Re\,\varepsilon^2} \equiv \frac{1}{\alpha Re\,\varepsilon^2}\int_0^1 u_y(y)dy = \frac{B^3}{1120\,(B+3)^5}\left(19B^2+209B+504\right)+O(\varepsilon^3) \quad (34)$$

is plotted versus the slip number B. Appreciable slip occurs in the range $1 < B < 100$ and slip may be considered as strong for $B < 1$. In conclusion, the unidirectionality assumption is valid when the flow is creeping and/or slip is strong.

In Fig. 4, the contours of the velocity in the flow direction for $B = \infty$ (no slip) and 1 (strong slip) with $Re = 0$, $\varepsilon = 0.1$, and $\alpha = 0.01$ are compared. Even though the contour patterns are similar, the main difference is that the range of the velocity values, which in the case of no-slip is the interval [0, 1.5], shrinks with slip. This is demonstrated in Fig. 5, where the velocity profiles at the inlet-, mid-, and outlet-planes are plotted for $B = \infty$ and 1 (moderate slip). In the extreme case of full slip, u_x is uniform and equal to unity at the channel exit.

The effect of the compressibility number ε on the contours of u_x for $Re = 0$, $\alpha = 0.01$ and $B = 1$ (strong slip) is illustrated in Fig. 6. The incompressible flow ($\varepsilon = 0$) is one-dimensional and thus the contour lines

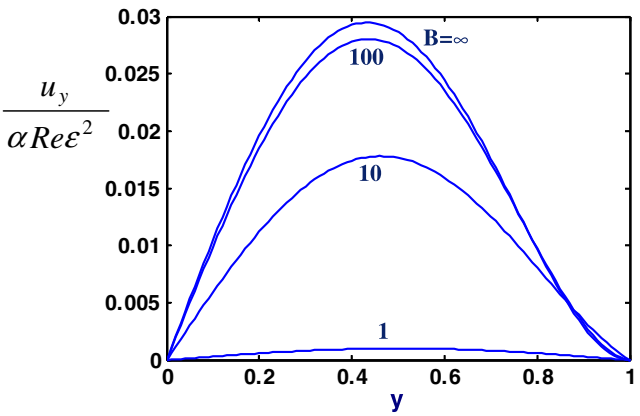

Fig. 2 Effect of the slip number on the transverse velocity component

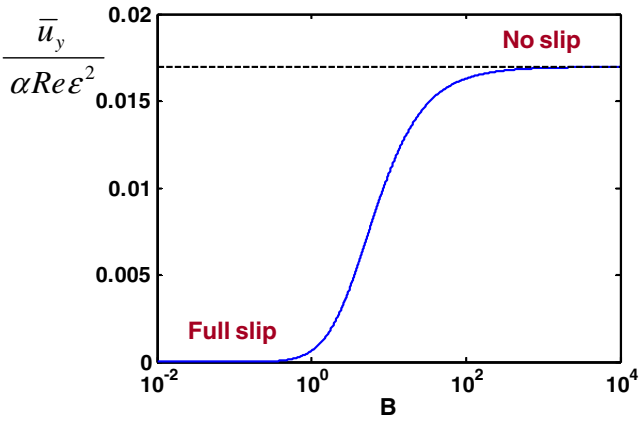

Fig. 3 The mean transverse velocity as a function of the slip number

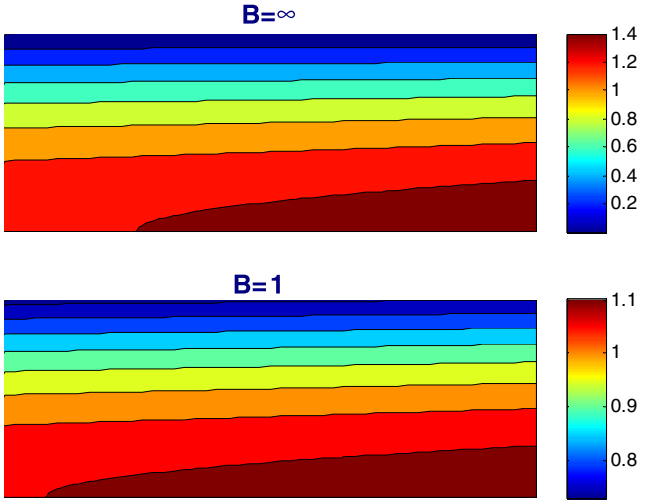

Fig. 4 Contours of u_x for $B = \infty$ (no slip) and 1 (strong slip); $Re = 0$, $\varepsilon = 0.1$, and $\alpha = 0.01$

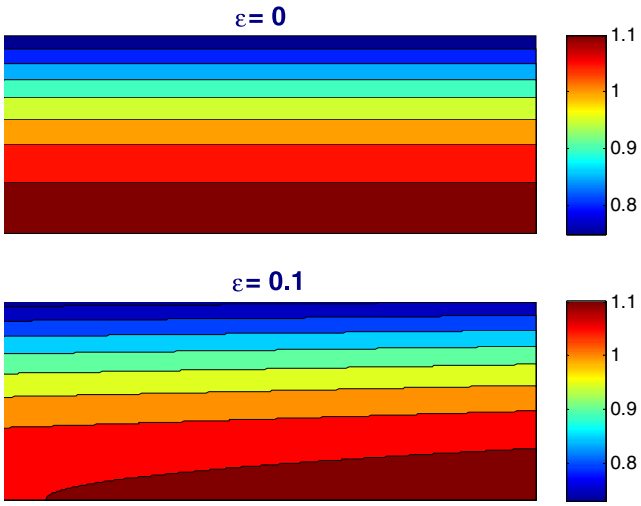

Fig. 6 Contours of u_x for $\varepsilon = 0$ (incompressible flow) and 0.1; $Re = 0$, $B = 1$ and $\alpha = 0.01$

are horizontal. In the case of compressible flow ($\varepsilon = 0.1$) fluid particles accelerate as they are decompressed downstream, due to the conservation of mass. As a result, the contours remain parallel only near the exit plane and tend towards the plane of symmetry upstream.

In Fig. 7, the velocity contours obtained with $Re = 0$ and 100 and $B = 1$, $\varepsilon = 0.1$, and $\alpha = 0.01$ are shown. The results are essentially the same, since higher-order contributions contain the product αRe which is small.

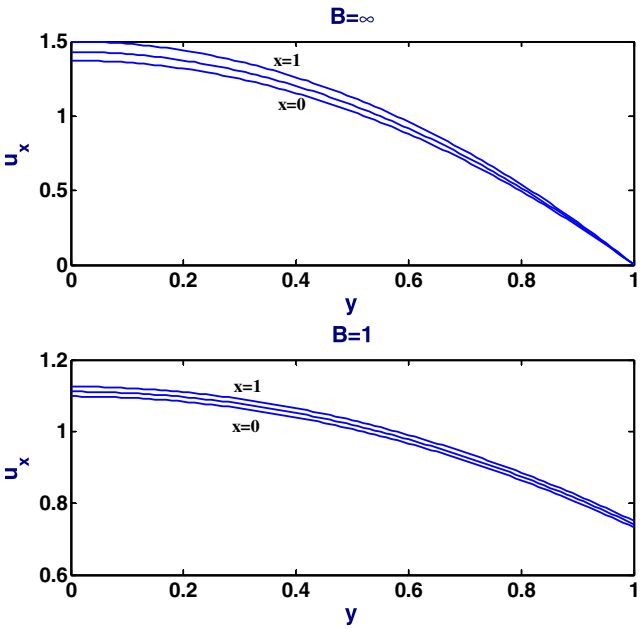

Fig. 5 Profiles of the velocity in the flow direction at $x = 0$, 0.5 and 1 for $B = \infty$ (no slip) and 1; $\varepsilon = 0.1$, $Re = 0$, and $\alpha = 0.01$

To magnify the effect of αRe, the velocity contours for a shorter channel with aspect ratio $\alpha = 0.1$ are plotted in Fig. 8. It is observed that the effect of Reynolds number becomes significant. The acceleration of the fluid particles within the slit increases with inertia. Note that, the Mach number corresponding to $Re = 100$, $\varepsilon = 0.1$, and $\alpha = 0.1$ is equal to 0.6 (γ is of unity order) and the flow can no longer be considered weakly compressible. However, the asymptotic expansions are still valid since the compressibility number is still small. Note that, since $Re = 3\,(\gamma/a\varepsilon)\,Ma^2$, when the compressibility number ε and the Mach number are small (<0.3), solutions are admissible only below

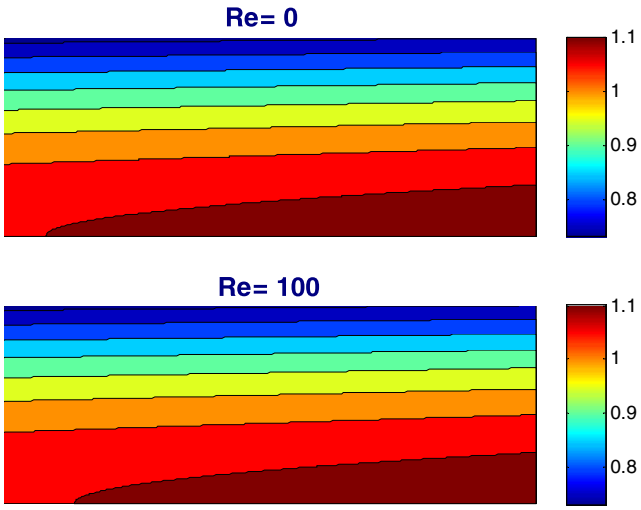

Fig. 7 Contours of u_x for $Re = 0$ and 100; $\alpha = 0.01$ (long channel), $B = 1$, and $\varepsilon = 0.1$

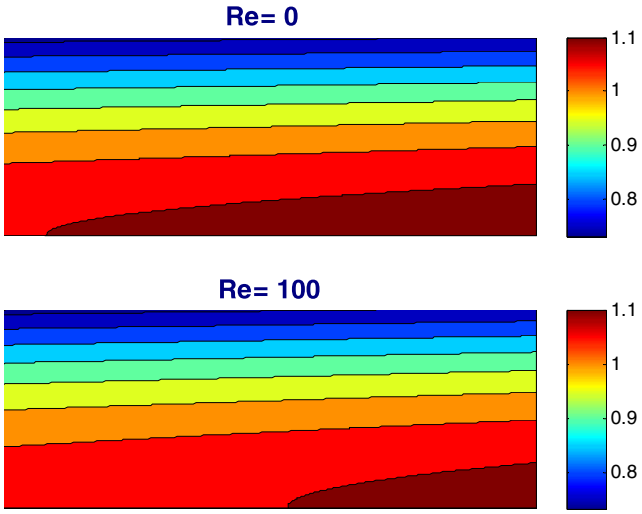

Fig. 8 Contours of u_x for $Re = 0$ and 100; $\alpha = 0.1$ (shorter channel), $B = 1$, and $\varepsilon = 0.1$

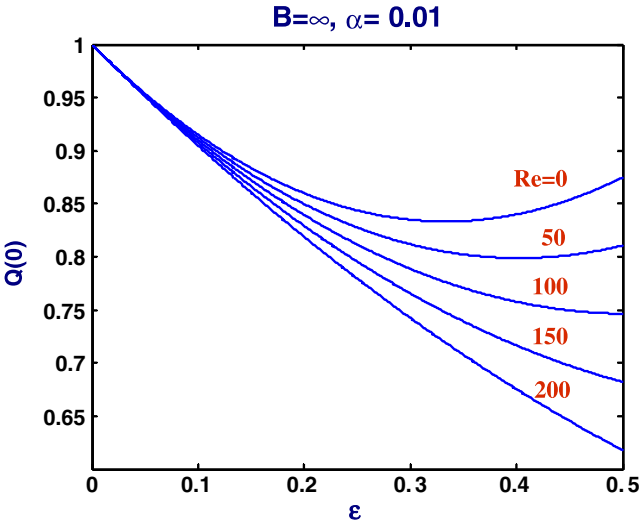

Fig. 9 The volumetric flow rate at the inlet plane for different Reynolds numbers with $\alpha = 0.01$ and no slip at the wall ($B = \infty$)

a critical value of the Reynolds number (for example, the critical value for Re is 270 for the data in Fig. 7 and is reduced to 27 in Fig. 8 where α is increased from 0.01 to 0.1). Generally, as the channel becomes shorter (α increasing) the admissible Reynolds numbers get smaller—the flow tends to creeping flow.

Another way to investigate the validity of our solution arises by looking into the volumetric flow rate given by Eq. 33. Since the solution is up to second order, Q is a parabolic function of ε for any value of x. At the exit plane,

$$Q(1) = 1 - \frac{\alpha^2 B^2 (2B+5)}{15 (B+3)^3} \varepsilon^2 + O(\varepsilon^3) \tag{35}$$

Obviously, $Q(1)$ is slightly below unity, given that $\alpha\varepsilon$ is small. Since the flow is compressible, the volumetric flow rate is reduced as we move upstream. A solution is assumed to be admissible if the volumetric flow rate $Q(0)$ at the inlet is a decreasing function of ε and positive. In Fig. 9, $Q(0)$ is plotted versus ε for various Reynolds numbers, with $B = \infty$ (no slip) and $\alpha = 0.01$. In creeping flow ($Re = 0$), solutions are admissible for $\varepsilon < 1/3$. As the Reynolds number is increased, $Q(0)$ decreases faster with ε and may become negative for even smaller compressibility numbers. In other words, given the compressibility number, the aspect ratio, and the Mach number, solutions are admissible only below a critical value of the Reynolds number, which has also be noted above. As shown in Fig. 10, slip weakens the compressibility effects and reduces the reduction of the volumetric flow rate upstream. As a result, slip extends the range of admissible solutions by shifting the minimum of $Q(0)$ to the right (Fig. 11).

From Eq. 31, we see that the density ρ at the exit plane is 1 at leading order. At the inlet plane, where the density obviously is maximized, we have

$$\rho(x = 0) = 1 + \frac{B}{B+3} \varepsilon + O(\varepsilon^2) \tag{36}$$

The maximum value for ρ, obtained in the case of no slip ($B = \infty$), is given by

$$\rho_{\max} = 1 + \varepsilon + O(\varepsilon^2) \tag{37}$$

and is independent of Re and α. In creeping flow, $\varepsilon < 1/3$ and thus the maximum admissible value of the density for any α is $\rho_{\max} = 4/3$, which restricts the range

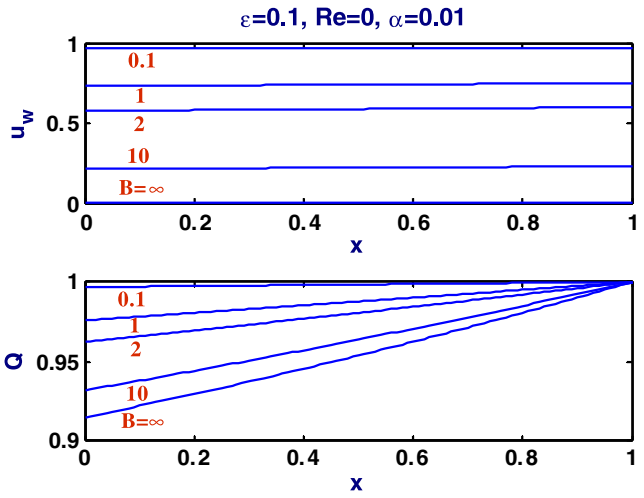

Fig. 10 Variations of the slip velocity and the volumetric flow in the channel for different slip numbers, $\varepsilon = 0.1$, $Re = 0$ and $\alpha = 0.01$

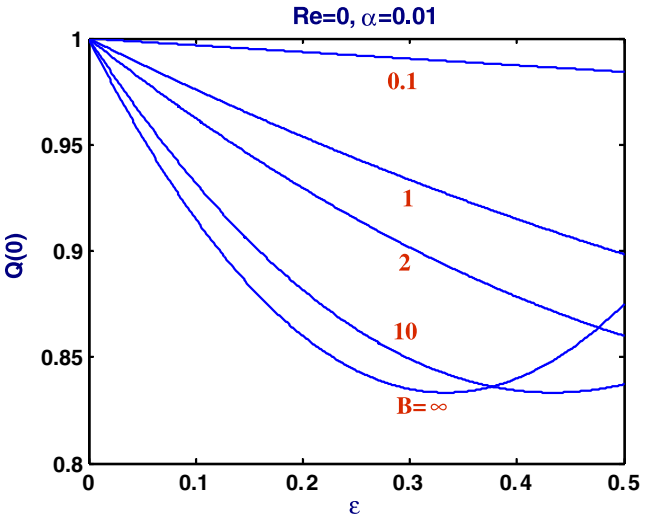

Fig. 11 Effect of slip number on the volumetric flow rate at the entrance plane; $Re = 0, \alpha = 0.01$

of validity of the solution. However, more compression, which is expected for very small values of α (for very long channels), can be obtained only if higher values of the compressibility number are admissible, i.e., for lower values of the Reynolds number. In other words, moderately compressible flow is associated with finite, moderate Reynolds numbers. Recalling that for weakly compressible flow we have $\alpha\varepsilon Re < 0.27$, such a combination of ε and Re is allowed only for smaller values of the aspect ratio α.

Generally, slip reduces the pressure in the channel and the required pressure drop. In Fig. 12, we show

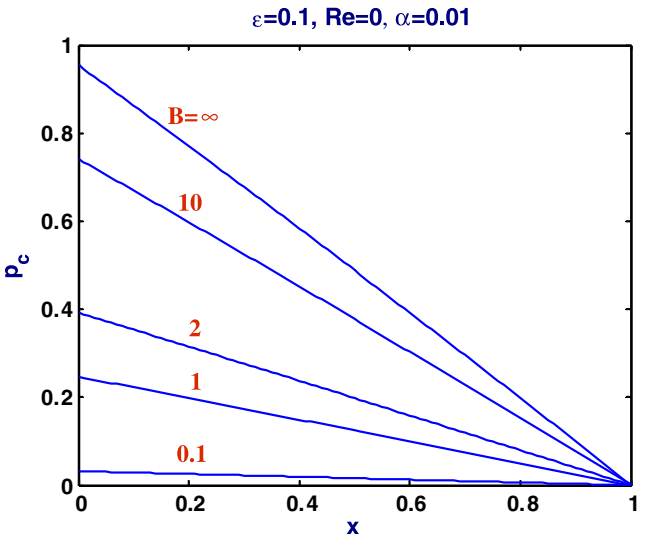

Fig. 12 Variation of the pressure along the centreline for various slip numbers; $\varepsilon = 0.1, Re = 0, \alpha = 0.01$

the distribution of the pressure along the centreline for different slip numbers, $\varepsilon = 0.1$, $Re = 0$ and $\alpha = 0.01$. As the slip number tends to zero (full slip) the pressure tends to become zero everywhere. Following Venerus and Bugajsky (2010) we calculate the mean pressure drop as follows

$$\overline{\Delta p} \equiv \overline{p}(0) - \overline{p}(1) \equiv \int_0^1 \left[p\,(0,\,y) - p\,(1,\,y)\right] dy \qquad (38)$$

which gives

$$\begin{aligned}\overline{\Delta p} = \frac{\overline{B}}{3} - \left[\frac{\overline{B}^2}{18} - \frac{\alpha Re\overline{B}^4}{315B^3}\left(2B^3+14B^2+35B+35\right)\right]\varepsilon \\ + \left[\frac{\overline{B}^3}{54} - \frac{2\alpha Re\overline{B}^5}{945B^3}\left(2B^3+14B^2+35B+35\right) - \frac{\alpha^2\overline{B}^4}{243B^2}\right. \\ \times \left(5B^2+25B+36\right) + \frac{\alpha^2 Re^2\bar{B}^7}{29469825B^6} \\ \times \left(3044B^6+42616B^5+267036B^4+951720B^3\right. \\ \left.\left. +1964655B^2+2182950B+1091475\right)\right]\varepsilon^2 \\ + O\left(\varepsilon^3\right)\end{aligned} \qquad (39)$$

Equation 39 gives the pressure drop for channel flow of a compressible Newtonian fluid with slip at the wall. This is a generalization of the result provided by Venerus and Bugajsky (2010) for the no-slip case ($B = \infty$):

$$\begin{aligned}\overline{\Delta p} = 1 - \left(\frac{1}{2} - \frac{18}{35}\alpha Re\right)\varepsilon \\ + \left(\frac{1}{2} - \frac{5}{3}\alpha^2 - \frac{36}{35}\alpha Re + \frac{3044}{13475}\alpha^2 Re^2\right)\varepsilon^2 + O\left(\varepsilon^3\right)\end{aligned} \qquad (40)$$

(It should be noted that the Reynolds number in Venerus and Bugajsky (2010) is twice the present Reynolds number.) It is clear that the required pressure drop decreases with compressibility and increases with inertia, as illustrated in Fig. 13. The effect of slip is illustrated in Fig. 14 where the pressure drops for various slip numbers are plotted. Slip leads to the reduction of the pressure difference required to drive the flow and consequently alleviates compressibility effects. This is, of course, expected and also noted in previous works. For example, Zhang et al. (2009), in their analysis of slip flow characteristics of compressible gases in microchannels, reported that "slip effect makes the flow less compressible". For the set of values used to construct Figs. 13 and 14, the wall and centerline pressures are essentially constant, i.e. the pressure is

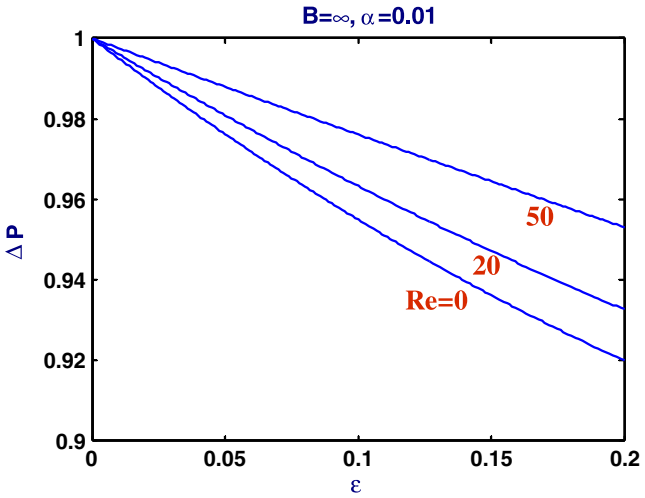

Fig. 13 Effect of the Reynolds number on the mean pressure drop; no slip, $\alpha = 0.01$

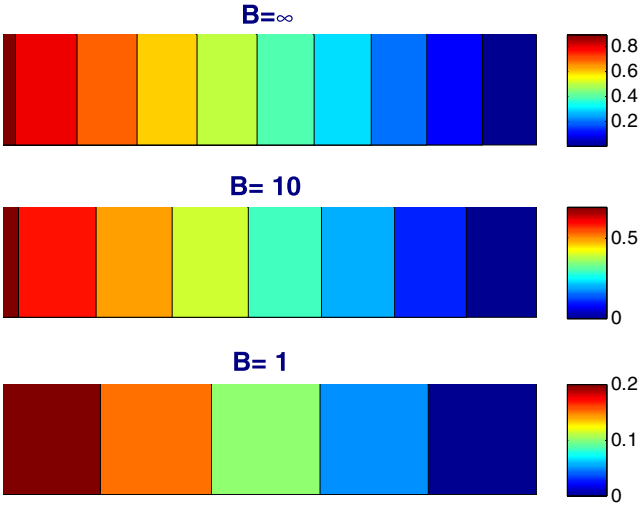

Fig. 15 Pressure contours for different slip numbers, $\varepsilon = 0.2$ $Re = 0$, and $\alpha = 0.01$ (long channel)

essentially a function of x. Hence, the pressure contours are practically straight lines, parallel to the inlet and exit planes (Fig. 15). This is not the case for short channels, e.g. when $\alpha = 1$, since the contributions of the higher-order terms become more important; this effect is illustrated in Fig. 16.

The mean pressure drop for axisymmetric Poiseuille flow of a compressible Newtonian fluid with slip at the wall, defined by

$$\overline{\Delta p} \equiv \overline{p}\,(0) - \overline{p}\,(1) \equiv 2\int_0^1 \left[p\,(0,z) - p\,(1,z)\right] r dr \quad (41)$$

is:

$$\overline{\Delta p} = \frac{\overline{B}}{8} - \left[\frac{\overline{B}^2}{128} - \frac{\alpha Re\overline{B}^3}{2048B^2}\left(B^2+4B+8\right)\right]\varepsilon + \left[\frac{\overline{B}^3}{1024} - \frac{\alpha Re\overline{B}^4}{8192B^2}\left(B^2+4B+8\right) - \frac{\alpha^2\overline{B}^4}{294912B^2} \times\left(49B^2+300B+576\right) + \frac{\alpha^2 Re^2\overline{B}^6}{14155776B^5} \times\left(2B^5+24B^4+171B^3+648B^2+1080B+864\right)\right]\varepsilon^2 + O\left(\varepsilon^3\right) \quad (42)$$

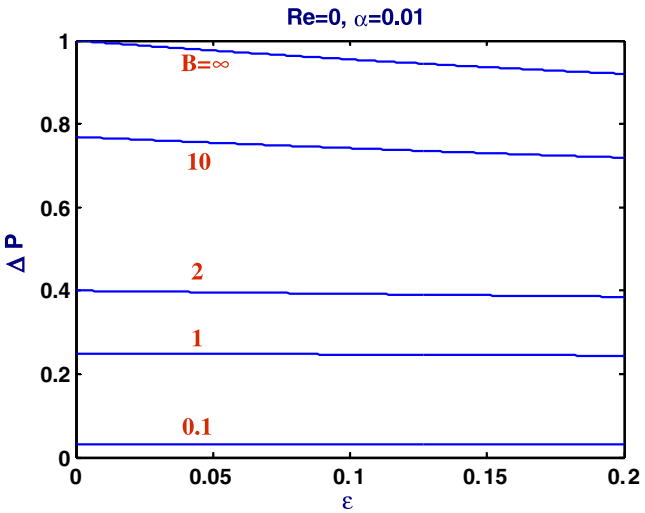

Fig. 14 Effect of the slip number on the mean pressure drop; $Re = 0$, $\alpha = 0.01$

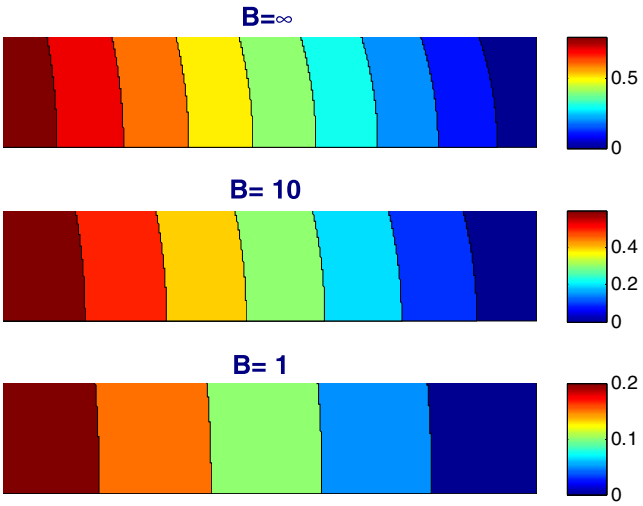

Fig. 16 Pressure contours for different compressibility numbers, $\varepsilon = 0.2$, $Re = 0$, and $\alpha = 1$ (short channel)

The above equation generalizes the result in Venerus (2006) for the no-slip case:

$$\overline{\Delta p} = 1 - \left(\frac{1}{2} - \frac{\alpha Re}{4}\right)\varepsilon + \left(\frac{1}{2} - \frac{\alpha Re}{2} - \frac{49\alpha^2}{72} + \frac{\alpha^2 Re^2}{27}\right)\varepsilon^2 + O\left(\varepsilon^3\right) \quad (43)$$

We have derived a solution for Eqs. 17–19 and 22–25 which is valid for all values of the channel aspect ratio α. It is, moreover, obvious from Eq. 19 that we recover the lubrication approximation ($\alpha^2 << 1$) with the transverse pressure gradient being zero when $\alpha Re << 1$ if all terms of order α^2 or higher are neglected (the aspect ratio α cannot be identically zero, since, in this limiting case, the pressure scale, i.e. the pressure required to drive the flow in a channel of infinite length with no slip at the wall, is infinite). Therefore, our solution gives the lubrication-theory solution in the presence of slip if we neglect the terms of order α^2 or higher and assume that $\alpha Re << 1$. The transverse velocity component vanishes, the pressure and the density are functions of x only, and the pressure drop is given by

$$\Delta p = \frac{\overline{B}}{3} - \frac{\overline{B}^2}{18}\varepsilon + \frac{\overline{B}^3}{54}\varepsilon^2 + O\left(\varepsilon^3\right) \quad (44)$$

The velocity in the flow direction is simplified to:

$$u_x = \frac{\overline{B}}{2B}\left(B + 2 - By^2\right) \times \left[1 - \frac{\overline{B}}{3}(1-x)\,\varepsilon + \frac{\overline{B}^2}{6}(1-x)^2\,\varepsilon^2\right] + O\left(\varepsilon^3\right) \quad (45)$$

As already discussed, such a solution is admissible if $Q(0)$ is a decreasing function of the compressibility number ε. This condition is satisfied when

$$\varepsilon < \frac{B+3}{3B} = \frac{1}{\overline{B}} \quad (46)$$

If a more refined solution is desired, one could construct perturbation expansions using α as the perturbation parameter (for any compressible flow) or double asymptotic expansions where both ε and α are perturbation parameters.

In the case of the axisymmetric Poiseuille flow, the average Darcy friction factor, defined by

$$\overline{f} \equiv -\frac{8}{Re}\int_0^1 \frac{\partial u_z}{\partial r}(1, z)\, dz \quad (47)$$

is of interest (Housiadas et al. 2012). Integrating the above equation yields

$$\frac{Re\,\overline{f}}{32} = \frac{B}{B+4} \times \left\{1 - \frac{B}{B+4}\left[\frac{1}{2} - \frac{B}{12\,(B+4)}\alpha Re\right]\varepsilon + \frac{B^2}{(B+4)^2} \times \left[\frac{1}{2} - \frac{13B+12}{72\,(B+4)}\alpha^2 - \frac{B^2+2B+4}{4B\,(B+4)}\alpha Re + \frac{17B^3+78B^2+360B+1440}{2160\,(B+4)^3}\alpha^2 Re^2\right]\varepsilon^2\right\} + O\left(\varepsilon^3\right) \quad (48)$$

In the no-slip limit ($B \to \infty$), one finds that

$$\frac{Re\,\overline{f}}{32} = 1 - \left(\frac{1}{2} - \frac{1}{12}\alpha Re\right)\varepsilon + \left(\frac{1}{2} - \frac{13}{72}\alpha^2 - \frac{1}{4}\alpha Re + \frac{17}{2160}\alpha^2 Re^2\right)\varepsilon^2 + O\left(\varepsilon^3\right) \quad (49)$$

Venerus (2006) compared the pressure drop and the friction factor for the no-slip case, defined respectively by Eqs. 43 and 49, and noted that the effect of inertia on pressure drop is significantly larger than on drag force. He also pointed out that the one-dimensional models for the no-slip case overpredict the

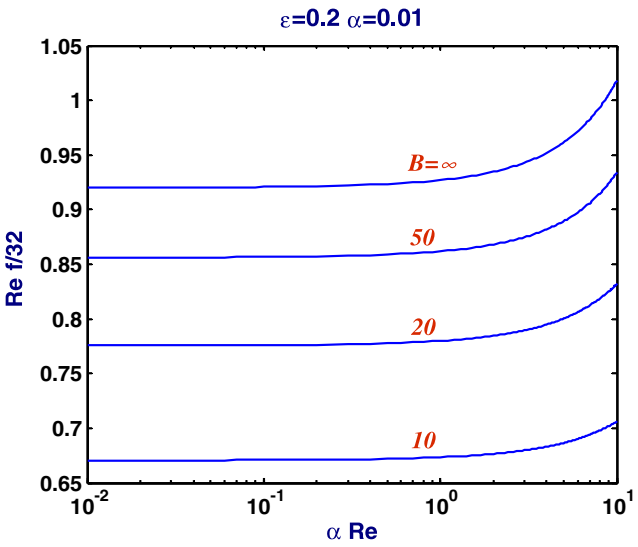

Fig. 17 The average Darcy friction factor for the axisymmetric Poiseuille flow versus αRe for various slip numbers; $\varepsilon = 0.2$ and $\alpha = 0.01$

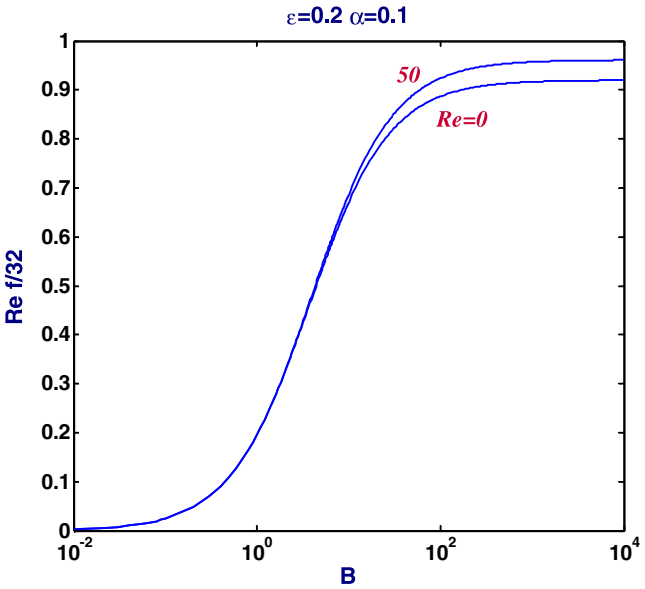

Fig. 18 Average Darcy friction factor for the axisymmetric Poiseuille flow versus the slip number for $Re = 0$ and 50; $\varepsilon = 0.2$ and $\alpha = 0.1$

friction factor by roughly 10%. Similarly to the pressure drop, the average Darcy friction factor is reduced dramatically with slip, as shown in Fig. 17. For a given slip number, it is essentially constant for a wide range of the parameter αRe corresponding to the weak compressibility regime and then increases rapidly. In Fig. 18, the average Darcy friction factor for $Re = 0$ and 50, $\varepsilon = 0.2$ and $\alpha = 0.1$ is plotted versus the slip number B. It can be seen that the friction factor is reduced with slip following a sigmoidal curve and also that the Reynolds number effect becomes weaker by slip.

Conclusions

We have derived perturbation solutions of the weakly compressible plane and axisymmetric Poiseuille flows with Navier's slip at the wall thus generalizing previous results by Taliadorou et al. (2009) and Venerus and Bugajsky (2010). The density is assumed to be a linear function of pressure and the associated isothermal compressibility number is used as the perturbation parameter. In the proposed derivation, the primary flow variables, i.e., the two velocity components, the pressure, and the density, are perturbed. Solutions have been obtained up to second order. The corresponding expressions of the volumetric flow rate and the pressure drop are also provided and discussed. As expected, slip weakens the y-dependence of the solution. The unidirectionality assumption is valid if the Reynolds number is very small and/or slip along the wall is strong. We are currently studying approximate solutions of weakly compressible Newtonian Poiseuille flows with pressure-dependent viscosity.

Appendix

In the case of compressible, axisymmetric Newtonian Poiseuille flow with slip at the wall, the perturbation solution is as follows:

$$
\begin{aligned}
u_z(r,z) = {} & \frac{\overline{B}}{4B}\left(B+2-Br^2\right) \\
& +\varepsilon\left[-\frac{\overline{B}^2}{32B}\left(B+2-Br^2\right)(1-z)+\frac{\alpha Re\overline{B}^4}{73728B^2}\left[-2\left(B^2+10B+24\right)+9\left(B^2+8B+16\right)r^2-9\left(B^2+6B+8\right)r^4+2\left(B^2+4B\right)r^6\right]\right] \\
& +\varepsilon^2\left[\frac{3\overline{B}^3}{512B}\left(B+2-Br^2\right)(1-z)^2-\frac{\alpha Re\overline{B}^5}{196608B^4}\right. \\
& \times\left[B^4+10B^3+72B^2+240B+192+6\left(B^4+8B^3+12B^2-16B\right)r^2-9\left(B^4+6B^3+8B^2\right)r^4+2\left(B^4+4B^3\right)r^6\right] \\
& \times(1-z)+\frac{\alpha^2\overline{B}^4}{294912B^2}\left[B^2+32B-48-4\left(7B^2+48B\right)r^2+27\left(B^4+4B^3\right)r^4\right]+\frac{\alpha^2Re^2\overline{B}^7}{459848300B^5} \\
& \times\left[43B^5+774B^4+1328B^3-42720B^2-268800B-460800-200\left(5B^5+80B^4+360B^3-96B^2-4032B-6912\right)r^2\right. \\
& +100\left(33B^5+462B^4+2112B^3+2736B^2-3456B-6912\right)r^4-1200\left(3B^5+36B^4+148B^3+224B^2+64B\right)r^6 \\
& \left.\left.+1425\left(B^5+10B^4+32B^3+32B^2\right)r^8-168\left(B^5+8B^4+16B^3\right)r^{10}\right]\right]+O\left(\varepsilon^3\right)
\end{aligned}
\tag{50}
$$

$$u_r(r) = \varepsilon^2 \frac{\alpha Re \overline{B}^5}{1179648 B^2} r\left(1-r^2\right)\left[4\left(B^2+10B+24\right)-\left(5B^2+32B+48\right)r^2+\left(B^2+4B\right)r^4\right]+O\left(\varepsilon^3\right) \quad (51)$$

$$\begin{aligned} p(r,z) = {} & \frac{\overline{B}}{8}(1-z)+\varepsilon\left[-\frac{\overline{B}^2}{128}(1-z)^2+\frac{\alpha Re\overline{B}^4}{16384B^3}\left(B^3+8B^2+24B+32\right)(1-z)+\frac{\alpha^2\overline{B}^2}{768}\left(1-r^2\right)\right] \\ & +\varepsilon^2\left[-\frac{\overline{B}^3}{1024}(1-z)^3-\frac{\alpha Re\overline{B}^5}{65536B^3}\left(B^3+8B^2+24B+32\right)(1-z)^2-\frac{\alpha^2\overline{B}^4}{147456B^2}\right. \\ & \times\left[29B^2+168B+228-9\left(B^2+4B\right)r^2\right](1-z)+\frac{\alpha^2Re^2\overline{B}^7}{113246208B^6} \\ & \times\left(2B^6+32B^5+267B^4+1332B^3+3672B^2+5184B+3456\right)(1-z)+\frac{\alpha^3Re\overline{B}^5}{14155776B^3} \\ & \times\left[19B^3+202B^2+576B+288-18\left(3B^3+24B^2+52B+16\right)r^2+45\left(B^3+6B^2+8B\right)r^4\right. \\ & \left.\left.-10\left(B^3+4B^2\right)r^6\right]\right]+O\left(\varepsilon^3\right) \end{aligned} \quad (52)$$

$$\rho(r,z) = 1+\varepsilon\frac{\overline{B}}{8}(1-z)+\varepsilon^2\left[-\frac{\overline{B}^2}{128}(1-z)^2+\frac{\alpha Re\overline{B}^4}{16384B^3}\left(B^3+8B^2+24B+32\right)(1-z)\frac{\alpha^2\overline{B}^2}{768}(1-r^2)\right]+O\left(\varepsilon^3\right) \quad (53)$$

In the above solution, z^* is scaled by the tube length L^*, r^* by the tube radius R^*, the axial velocity by $U^* = \dot{M}^*/\left(\pi\rho_0^* R^{*2}\right)$, the radial velocity by $U^* R^*/L^*$, and the pressure by $8\eta^* L^* U^*/R^{*2}$. The dimensionless numbers are defined as follows:

$$\alpha \equiv \frac{R^*}{L^*}, \quad Re \equiv \frac{\rho_0^* U^* R^*}{\eta^*}, \quad \varepsilon \equiv \frac{8\kappa^*\eta^* L^* U^*}{R^{*2}},$$

$$B \equiv \frac{\beta^* R^*}{\eta^*}, \quad \overline{B} \equiv \frac{8B}{B+4} \quad (54)$$

The volumetric flow rate,

$$Q(z) \equiv 2\int_0^1 u_z(r,z)\, r dr \quad (55)$$

is given by

$$\begin{aligned} Q(z) = {} & 1-\varepsilon\frac{\overline{B}}{8}(1-z) \\ & +\varepsilon^2\left[\frac{3\overline{B}^2}{128}(1-z)^2-\frac{\alpha Re\overline{B}^3}{2048B^2}\left(B^2+4B+8\right)(1-z)\right. \\ & \left.-\frac{\alpha^2\overline{B}^3}{9216B}(B+3)\right]+O\left(\varepsilon^3\right) \end{aligned} \quad (56)$$

For $\varepsilon = 0$ the standard fully-developed Poiseuille flow solution with slip at the wall is recovered with

$$u_z(r) = \frac{\overline{B}}{2B}+\frac{\overline{B}}{4}\left(1-r^2\right) \quad (57)$$

References

Arkilic EB, Schmidt MA (1997) Gaseous slip flow in long microchannels. J MEMS 6:167–178

Beskok A, Karniadakis GE (1999) Simulation of heat and momentum transfer in complex micro-geometries. J Thermophys Heat Transfer 8:355–377

Denn MM (2001) Extrusion instabilities and wall slip. Ann Rev Fluid Mech 33:265–287

Dubbeldam JLA, Molenaar J (2003) Dynamics of the spurt instability in polymer extrusion. J Non-Newton Fluid Mech 112:217–235

Felderhof BU, Ooms G (2011) Flow of a viscous compressible fluid produced in a circular tube by an impulsive point source. J Fluid Mech 668:100–112

Georgiou G (2005) Stick-slip instability. Chapter 7. In: Hatzikiriakos SG, Migler K (eds) Polymer processing instabilities: control and understanding. Mercel Dekker, Inc., pp 161–206

Georgiou GC, Crochet MJ (1994) Compressible viscous flow in slits with slip at the wall. J Rheol 38:639–654

Guaily A, Cheluget E, Lee K, Epstein M (2011) A new hyperbolic model and an experimental study for the flow of polymer melts in multi-pass rheometer. Comp Fluids 44:258–266

Hatzikiriakos SG (2012) Wall slip of molten polymers. Progr Polym Sci 37:624–643

Hatzikiriakos SG, Dealy JM (1992) Role of slip and fracture in the oscillating flow of a HDPE in a capillary. J Rheol 36:845–884

Hatzikiriakos SG, Dealy JM (1994) Start-up pressure transients in a capillary rheometer. Polym Eng Sci 34:493–499

Hatzikiriakos SG, Migler K (2005) Polymer processing instabilities: control and understanding. Mercel Dekker, New York

Housiadas K, Georgiou GC (2011) Perturbation solution of Poiseuille flow of a weakly compressible Oldroyd-B fluid. J Non-Newton Fluid Mech 166:73–92

Housiadas KD, Georgiou GC, Mamoutos IG (2012) Laminar axisymmetric flow of a weakly compressible viscoelastic fluid. Rheol Acta doi:10.1007/s00397-011-0610-x

Kohl MJ, Abdel-Khalik SI, Jeter SM, Sadowski DL (2005) An experimental investigation of microchannel flow with internal pressure measurements. Int J Heat Mass Transfer 48:1518–1533

Mitsoulis E, Hatzikiriakos SG (2009) Steady flow simulations of compressible PTFE paste extrusion under severe wall slip. J Non-Newton Fluid Mech 157:26–33

Piau JM, El Kissi N (1994) Measurement and modelling of friction in polymer melts during macroscopic slip at the wall. J Non-Newton Fluid Mech 54:121–142

Poyiadji S (2012) Flows of fluids with pressure-dependent material properties. PhD Thesis, University of Cyprus

Qin FH, Sun DJ, Yin XY (2007) Perturbation analysis on gas flow in a straight microchannel. Phys Fluids 19:027103

Stone HA, Stroock AD, Ajdari A (2004) Engineering flows in small devices: microfluidics toward a lab-on-a-chip. Annu Rev Fluid Mech 36:381–411

Taliadorou E, Georgiou E, Alexandrou AN (2007) A two-dimensional numerical study of the stick-slip extrusion instability. J Non-Newton Fluid Mech 146:30–44

Taliadorou E, Georgiou GC, Mitsoulis E (2008) Numerical simulation of the extrusion of strongly compressible Newtonian liquids. Rheol Acta 47:49–62

Taliadorou E, Neophytou M, Georgiou GC (2009) Perturbation solutions of Poiseuille flows of weakly compressible Newtonian liquids. J Non-Newton Fluid Mech 158:162–169

Tang HS, Kalyon DM (2008a) Unsteady circular tube flow of compressible polymeric liquids subject to pressure-dependent wall slip. J Rheol 52:507–525

Tang HS, Kalyon DM (2008b) Time-dependent tube flow of compressible suspensions subject to pressure-dependent wall slip: ramifications on development of flow instabilities. J Rheol 52:1069–1090

Venerus DC (2006) Laminar capillary flow of compressible viscous fluids. J Fluid Mech 555:59–80

Venerus DC, Bugajsky DJ 2010 Laminar flow in a channel. Phys Fluids 22:046101

Vinay G, Wachs A, Frigaard I (2006) Numerical simulation of weakly compressible Bingham flows: the restart of pipeline flows of waxy crude oils. J Non-Newton Fluid Mech 136:93–105

Wachs A, Vinay G, Frigaard I (2009) A 1.5D numerical model for the start up of weakly compressible flow of a viscoplastic and thixotropic fluid in pipelines. J Non-Newton Fluid Mech 159:81–94

Zhang TT, Jia L, Wang ZC, Li CW (2009) Slip flow characteristics of compressible gaseous in microchannels. Energy Conv Manage 50:1676–1682